

Spectral/Energy Efficiency Tradeoff of Cellular Systems With Mobile Femtocell Deployment

Fourat Haider, Cheng-Xiang Wang, *Senior Member, IEEE*, Bo Ai, *Senior Member, IEEE*, Harald Haas, *Member, IEEE*, and Erol Hepsaydir

Abstract—The mobile femtocell (MFemtocell) is a new concept that has been recently proposed to be a potential wireless communication technology for next-generation cellular systems. The essence of MFemtocell lies in adopting the femtocell technology inside vehicles such as trains, buses, or private cars to provide better coverage and a good Internet experience while on the move. In this paper, we investigate the spectral and energy efficiency for the MFemtocell-assisted network with different resource partitioning schemes. Closed-form expressions for the relationships between spectral efficiency and energy efficiency are derived for a link-level MFemtocell network. We also investigate the spectral efficiency for multiuser system-level MFemtocells with opportunistic scheduling schemes. Our analysis shows that MFemtocells can provide better spectral and energy efficiency compared with the direct transmission scheme.

Index Terms—Energy efficiency, mobile femtocell (MFemtocell), resource partitioning schemes, scheduling schemes, spectral efficiency.

I. INTRODUCTION

HETEROGENEOUS network (HetNet) deployments are seen as a promising solution for cellular operators to improve indoor coverage and increase spectral efficiency with low operational expense (OPEX) [1]. In fact, a HetNet is considered crucial for mobile data offloading and will become an essential part of next-generation cellular systems [2]. One key component in HetNets is femtocell technology. Femtocells are low-range low-power mobile base stations (BSs) that improve coverage inside a home or an office building [3]. They use

Manuscript received March 27, 2014; revised October 22, 2014 and February 11, 2015; accepted May 14, 2015. Date of publication June 10, 2015; date of current version May 12, 2016. This work was supported in part by the EU H2020 ITN 5G Wireless Project under Grant 641985, by the EU FP7 QUICK Project under Grant PIRSES-GA-2013-612652, by the National Natural Science Foundation of China under Grant 61222105, by the China 863 Project in 5G under Grant 2014AA01A706, by Hutchison 3G U.K., and by the Engineering and Physical Sciences Research Council under Grant EP/K008757/1. The review of this paper was coordinated by Dr. J. Pan.

F. Haider and C.-X. Wang are with the Joint Research Institute for Signal and Image Processing, School of Engineering and Physical Sciences, Heriot-Watt University, Edinburgh EH14 4AS, U.K. (e-mail: fsh12@hw.ac.uk; cheng-xiang.wang@hw.ac.uk).

B. Ai is with the State Key Laboratory of Rail Traffic Control and Safety, Beijing Jiaotong University, Beijing 100044, China (e-mail: boai@bjtu.edu.cn).

H. Haas is with the Joint Research Institute for Signal and Image Processing, Institute for Digital Communications, University of Edinburgh, Edinburgh EH9 3JL, U.K. (e-mail: h.haas@ed.ac.uk).

E. Hepsaydir is with Hutchison 3G U.K., Maidenhead SL6 1EH, U.K. (e-mail: erol.hepsaydir@three.co.uk).

Color versions of one or more of the figures in this paper are available online at <http://ieeexplore.ieee.org>.

Digital Object Identifier 10.1109/TVT.2015.2443046

broadband networks as backhaul to carry the traffic to the operator's data center. Femtocell technology has proven its excellent capability of grabbing indoor traffic from the macrocell layer and, thus, enables the latter to focus its attention toward outdoor traffic. Moreover, femtocell technology is considered as an energy-efficient solution due to its ability to achieve a high data rate with low transmit power due to the short distances toward its users [4].

Public vehicles, e.g., trains and buses, are moving hotspots with many people potentially requesting diverse data services, e.g., web browsing, video streaming, and gaming. Users inside a moving vehicle may execute multiple handovers at the same time, causing a significant increase in signaling load and high connection failures in the network. Furthermore, the vehicle may have a high penetration loss through its metallic enclosure, resulting in a poor network connection. Therefore, it is important to minimize the signaling load and drop calls within a fast-moving vehicle while providing a better Internet experience on the move. To this end, adopting femtocell technology inside a vehicle has inspired the evolution of a new concept called mobile femtocell (MFemtocell) [5]. MFemtocell is a mobile small cell that can dynamically change its connection to the operator's core network. The MFemtocell can be deployed on public transport buses, trains, and even private cars. The MFemtocell concept has been nominated to play a role in the fifth-generation (5G) cellular systems [6].

The implementation of MFemtocells can potentially benefit cellular networks. In this context, various research efforts have been made to study and appraise the operation of MFemtocell deployments [7]–[12]. For instance, Elkourdi and Simeone in [7] studied the performance advantage of using MFemtocell by communicating with the macro BS to improve and extend coverage for users. The potential advantages of using moving cells to boost performance for user equipments (UEs) in transit vehicles were highlighted in [8]. The MFemtocells can contribute to signaling overhead reduction in the network and improve the system performance [9]. The MFemtocell can also perform handover on behalf of all its associated users. This would reduce the number of handover attempts as the users move between cells in the network. The outage performance can also be improved in a high-speed mobility environment by using MFemtocells [10]. Due to a shorter communication range with the MFemtocell, the battery life of associated users would significantly increase. Qutqut, in [11, pp. 53–73], investigated an appropriate precoder at the MFemtocell in the vehicle to overcome the degraded performance of the received signal in outdoor wireless links. The proposed precoder helps in extracting

the underlying rich multipath Doppler diversity inherited in this type of double-selective fading link. Moreover, since the MFemtocells are located inside vehicles with antennas located outside the vehicle, this setup improves the signal quality inside the vehicle by avoiding the penetration loss. In addition, a larger number of antennas can be utilized at the MFemtocell with significant diversity/multiplexing gain. Last, but not least, the MFemtocell is multioperator friendly, which means that many operators can share the same MFemtocell, which forwards the traffic to the desired core network. The multioperator core network solution is commonly used for macro BSs [13].

To utilize the MFemtocell to its full advantage, one must overcome challenges, such as finding the most reliable backhaul to carry the traffic between the core network and MFemtocells' users, developing a strategy for sharing the spectrum between the macro BS and MFemtocells, and optimizing spectral and energy efficiency. Finding the most reliable backhaul methods, while maintaining good Internet-based user experience, is the greatest challenge that the MFemtocell concept faces. One way to achieve this is to use the standardized cellular air interface as a backhaul link, thus creating a similar situation as the concept of the mobile relay [14]–[17]. In this case, an MFemtocell behaves as a femtocell when serving its users and as a regular user when communicating with the macro BS. Furthermore, the traffic of users within an MFemtocell would be treated as single-user traffic when sending to or receiving from the MFemtocell over the air interface. MFemtocell is also able to adopt other backhaul methods for carrying the traffic, such as using a different radio access technology (e.g., Wi-Fi [12] or satellite) on a different spectrum. These options will enable more reliability in case that the serving macro BS is broken down due to failures and/or high congestion. Under these failure situations, a group of MFemtocells within close proximity will be able to create a new network layer, and by adopting different backhaul methods, the system can maintain the connectivity between the core network and the users. This offers a solution to the challenge that is posed during an emergency situation where the standard networks are jammed.

Regarding the second challenge of how to share the spectrum between the macro BS and the MFemtocell, we can examine the research on femtocell-based cellular systems. In this context, the femtocell can share the same spectrum with a macro BS (i.e., nonorthogonal transmission scheme) or utilize a dedicated spectrum (i.e., orthogonal transmission scheme) [18]–[21]. Using the same spectrum would improve spectrum utilization but contribute to additional interference for indoor and outdoor users. In an orthogonal transmission scheme, the femtocell uses a dedicated spectrum band that is not used by a macro network. This mode eliminates the mutual interference between the femtocell and the macro BS, i.e., intracell interference. However, additional spectrum resources are required, and this may have a negative impact on spectrum utilization.

The third challenge is related to the energy-efficient communication, or what is globally well known as Green Radio [22]. This issue has been attracting increasing attention in various societies. This is because the increase of energy consumption in wireless communication systems has indirectly caused a rise in the emission of CO₂, which is currently considered to be a

major threat to the environment. Jointly attaining both enhanced energy efficiency, i.e., the required energy per bit, and spectral efficiency, i.e., the number of bits per second transmitted over a given bandwidth, is a challenging problem to solve. Unfortunately, achieving an enhancement of one of them often means sacrificing the other. Therefore, it is important to study different tradeoffs between the two performance indicators to decide on the minimum energy consumption that is required to achieve the target spectral efficiency, or *vice versa* [23]–[26]. Two analytical methods to analyze the spectral/energy efficiency tradeoff were proposed in [27] and [28] for low and high signal-to-noise ratio (SNR) regimes, respectively. These tools have been adopted in a variety of network scenarios. For the low-SNR regime tool introduced in [27], the relationship between the energy and spectral efficiencies was studied for single-user multiple-input–multiple-output channels [29], single-user relay channels [30]–[32], and multiuser scenarios [33]. Jindal in [34] and Lozano *et al.* in [35] used the high-SNR regime tool to analyze the energy efficiency in multiantenna channels. The low- and high-SNR tools were also used to investigate the spectral/energy efficiency tradeoff for cognitive radio networks [36]. To the best of our knowledge, no existing work has investigated the spectral/energy efficiency tradeoff in MFemtocell networks. Therefore, the main contributions of this paper are summarized as follows.

- 1) We investigate the spectral/energy efficiency tradeoff for MFemtocell networks. Closed-form expressions for the relationships between the energy efficiency and the spectral efficiency are derived in low- and high-SNR regimes for a link-level MFemtocell with two different resource partitioning (i.e., orthogonal and nonorthogonal) schemes.
- 2) We also present a spectral efficiency analysis of system-level MFemtocells with orthogonal frequency-division multiple access (OFDMA)-based spectrum reuse and opportunistic scheduling schemes.

The rest of this paper is organized as follows. Section II describes the MFemtocell system model and two resource partitioning schemes. In Section III, the relationship between energy efficiency and spectral efficiency is analyzed for a link-level MFemtocell with two different resource partitioning schemes. Section IV investigates the spectral efficiency of a system-level MFemtocell network with multiusers and opportunistic scheduling schemes. Finally, Section V concludes this paper.

II. MOBILE FEMTOCELL SYSTEM MODEL AND RESOURCE PARTITIONING SCHEMES

Let us consider an MFemtocell-assisted cellular network shown Fig. 1 with a single BS, multiple MFemtocells, and multiple users. The MFemtocell set is denoted by $\mathcal{J} = \{1, \dots, J\}$. The total of U users, which is given by the set $\mathcal{U} = \{1, \dots, U\}$, is divided into two categories: direct transmission and access users. Let $\mathcal{N} = \{1, \dots, N\}$ denote the set of users that communicate directly with the BS. Furthermore, there is the set $\mathcal{M}_j = \{1, \dots, M_j\}$ of access users that communicate through MFemtocell $j \in \mathcal{J}$. Both M_j and N can be variables;

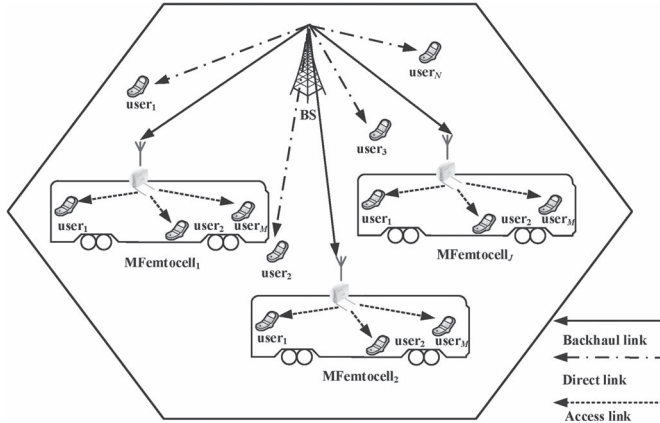


Fig. 1. System model. Single cell with multiple MFemtocells and users.

however, $\sum_{j=1}^J M_j + N = U$. The index of the BS is assumed to be zero and, therefore, is omitted from the analysis. We assume a relaying-based backhauling in which the MFemtocells are using the same standardized air interface to carry the traffic from the BS. The terms backhaul link, access link, and direct link are used to denote BS–MFemtocell, MFemtocell–user, and BS–user links, respectively. We assume that the backhaul, access, and direct links all experience non-line-of-sight Rayleigh block-fading channels, which are kept constant within a sub-frame and change independently in the following subframe. We also assume that the backhaul link has a gain G over the direct link. This gain can be achieved by using a highly directional antenna pattern as well as pointing MFemtocell’s antenna toward the BS.

A. Resource Partitioning Schemes

By adopting the MFemtocell, the spectrum has to be allocated (or reused) among different links, i.e., the backhaul, direct, and access links. It is essential to design an efficient resource partitioning policy in the MFemtocell-enhanced system to improve the performance of the whole system. We assume a time-division relaying-based backhauling scheme, in which the transmission to the end users occurs in two time periods. Each time period contains a specific number of time slots. The BS will transmit traffic to MFemtocells over backhaul links in the first time period. In the second time period, the BS and the MFemtocell are simultaneously communicating to the direct transmission and access users, respectively, using either an orthogonal or a nonorthogonal transmission scheme. The two resource partitioning policies are explained as follows.

1) *Orthogonal Resource Partitioning Scheme:* In this scheme, the radio resources allocated to the backhaul, direct, and access links are all orthogonal either in the time or the frequency domain, and hence, there is no intracell interference from the BS to the MFemtocell users, and *vice versa*. In this scheme, a fraction β ($0 < \beta < 1$) of the spectrum is exclusively allocated for direct transmissions while the rest of the spectrum is allocated to the access transmission, as presented in Fig. 2(a). The interference from an MFemtocell to the access users of other MFemtocells can be neg-

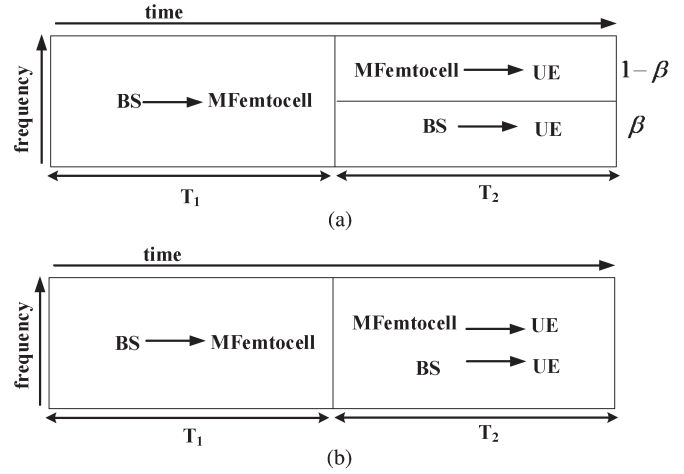


Fig. 2. Two different resource partitioning schemes for MFemtocell. (a) Orthogonal resource partitioning scheme. (b) Nonorthogonal resource partitioning scheme.

ligible or considered as background noise. This is because signals that come from an MFemtocell should travel through at least two metallic enclosures to reach the other MFemtocell users. The instantaneous faded SNR for the direct transmission user $n \{n \in \mathcal{N}\}$ and access user $m_j \{m_j \in \mathcal{M}_j\}$ can be calculated by

$$\gamma_d(n) = \frac{|h_d(n)|^2 P_{BS}}{BN_0}, \quad n \in \mathcal{N} \quad (1)$$

$$\gamma_a(j, m_j) = \frac{|h_a(j, m_j)|^2 P_{MF}}{BN_0}, \quad m_j \in \mathcal{M}_j \quad (2)$$

respectively, where $h_d(n)$ and $h_a(j, m_j)$ are complex-valued channel gains over the direct link and the access link, respectively; P_{BS} and P_{MF} are the BS and MFemtocell transmit power values, respectively; B is the system bandwidth; and N_0 is noise spectral density.

2) *Nonorthogonal Resource Partitioning Scheme:* In this scheme, the radio resources are reused by the direct and access links, as shown in Fig. 2(b). However, the radio resources are still orthogonally allocated between backhaul and direct links and between backhaul and access links. Nonorthogonal mode means that there will be intracell interference to the access and direct transmission users due to the simultaneous transmissions from MFemtocell and the BS on the same spectrum. The advantage of this scheme is the improvement in resource utilization compared with the orthogonal scheme. In addition, this scheme gives the flexibility to implement radio resource management at the BS and the MFemtocell independently. The instantaneous received signal-to-interference-plus-noise ratio (SINR) for a direct transmission user, which is denoted by $\hat{\gamma}_d(n)$, can be calculated as

$$\hat{\gamma}_d(n) = \frac{|h_d(n)|^2 P_{BS}}{I + BN_0}, \quad n \in \mathcal{N} \quad (3)$$

where I is the intracell interference generated from all the MFemtocells. This type of interference can be scaled down significantly by the indoor penetration loss, as well as by

constraining the transmit power within the MFemtocell using a directive antenna. On the other hand, the received SINR for an access-link user is given by

$$\begin{aligned}\hat{\gamma}_a(j, m_j) &= \frac{|h_a(j, m_j)|^2 P_{\text{MF}}}{|h_d(m_j)|^2 P_{\text{BS}} + BN_0} \\ &= \frac{\gamma_a(j, m_j)}{\gamma_d(j, m_j) + 1}, \quad m_j \in \mathcal{M}_j.\end{aligned}\quad (4)$$

Hence, $\hat{\gamma}_a(j, m_j)$ can be characterized by the instantaneous SNR received from an MFemtocell, $\gamma_a(j, m_j)$ in (2), and the achieved SNR if the same user is served by the BS instead, i.e., $\gamma_d(j, m_j)$. Again, the interference between MFemtocells is negligible or considered as background noise. Now, if we assume that the distance between an MFemtocell and the BS and the distance between the MFemtocell's users and the BS are approximately the same, then (4) can be rewritten as

$$\hat{\gamma}_a(j, m_j) \approx \frac{\gamma_a(j, m_j)}{\frac{\gamma_b(j)}{G} + 1}, \quad m \in \mathcal{M}_j \quad (5)$$

where G is the backhaul gain over the direct transmission link. In (5), $\gamma_b(j)$ is the SNR for a backhaul channel of MFemtocell j and can be calculated as

$$\gamma_b(j) = \frac{|h_b(j)|^2 P_{\text{BS}}}{BN_0}, \quad j \in \mathcal{J} \quad (6)$$

where $h_b(j)$ denotes the complex-valued channel gain of the backhaul link for MFemtocell j .

III. SPECTRAL/ENERGY EFFICIENCY TRADEOFF FOR A LINK-LEVEL MOBILE FEMTOCELL

Here, the spectral/energy efficiency tradeoff is studied for a link-level MFemtocell network in low- and high-SNR regimes. The system we are interested in here consists of the BS, a single MFemtocell, and a user. For notational convenience, the user and MFemtocell indexes will be omitted as well since we are dealing with link-level performance. The channel gains will be denoted by h_d , h_b , and h_a for direct, backhaul, and access links, respectively. The energy efficiency here is defined as the required energy per bit (in joules per bit) normalized to the background noise spectral level, i.e., (E_b/N_0) , for reliable communication. The spectral efficiency refers to the number of bits per second transmitted over a given bandwidth (in bits per second per hertz). The MFemtocell will receive the data in T_1 and then transmit the data again to the user in T_2 . For simplicity and without loss of generality, both T_1 and T_2 are assumed to be equal to one time slot. For a fair comparison, the transmit power and total bandwidth are set to be the same for cases with or without MFemtocell deployment. Thus, the total transmit power P over the two time slots is shared between the BS and the MFemtocell. The transmit power from the BS is then given by

$$P_{\text{BS}} = \alpha P \quad (7)$$

and the remaining power, i.e., P_{MF} , will be allocated to the MFemtocell and is given by

$$P_{\text{MF}} = (1 - \alpha)P. \quad (8)$$

Therefore, in the case without MFemtocell deployment, the BS is able to serve users with full transmit power, i.e., $\alpha = 1$. In addition, it has been assumed that the same size of bandwidth is used in T_1 and T_2 .

A. Low-SNR Regime

In the low-SNR regime, (E_b/N_0) can be approximated as an affine function with respect to the spectral efficiency and can be expressed as [27]

$$\left(\frac{E_b}{N_0}\right) \Big|_{\text{dB}} = \left(\frac{E_b}{N_0}\right)_{\min} + \frac{3}{S_0}C \quad (9)$$

where $(E_b/N_0)_{\min}$ is the minimum energy efficiency required for transmitting information reliably over a channel, and it is given by

$$\left(\frac{E_b}{N_0}\right)_{\min} = \lim_{\text{SNR} \rightarrow 0} \frac{\text{SNR}}{C(\text{SNR})}. \quad (10)$$

Here, $C(\text{SNR})$ is the spectral efficiency as a function of $\text{SNR} = P/BN_0$. In (9), S_0 is the wideband slope of the spectral efficiency, which is defined as the increase in bits per second per hertz per 3 dB [b/s/Hz/(3 dB)], and can be expressed as [27]

$$S_0 = \frac{2\dot{C}(0)}{-\ddot{C}(0)} \quad (11)$$

where $\dot{C}(0)$ and $\ddot{C}(0)$ are the first and second derivatives, respectively, when $\text{SNR} \equiv 0$. We use the notation C and C to distinguish between the spectral efficiency as a function of SNR and as a function of (E_b/N_0) , respectively.

- Direct transmission scheme:

Let us first analyze the required normalized energy per bit for the direct transmission scheme that will be used later as a reference. Here, we assume that the BS is communicating directly with a user without the assistance of an MFemtocell. For the direct transmission scheme with a Rayleigh fading channel, the relationship between (E_b/N_0) and the direct spectral efficiency C^{direct} is given by

$$\left(\frac{E_b}{N_0}\right)_{\text{dB}}^{\text{direct}} \approx -1.59 + 10 \log_{10}(A_d) + 3C^{\text{direct}} \quad (12)$$

where A_d denotes the mean power of the direct transmission channel.

Proof: See Appendix A. ■

- Orthogonal scheme:

In this scenario, we assume that a user is communicating with the MFemtocell rather the BS. However, the MFemtocell will receive and buffer the data in T_1 from the BS and serve the

user in T_2 . In this case, the required (E_b/N_0) to achieve the spectral efficiency of the orthogonal scheme, i.e., C^{orthg} , in the low-SNR regime can be given by

$$\left(\frac{E_b}{N_0}\right)_{\text{dB}}^{\text{orthg}} \approx 10 \log_{10} \left(\frac{2 \ln 2}{\alpha G A_d} \right) + 2C^{\text{orthg}} \times 10 \log_{10} 2 \quad (13)$$

where α ($0 < \alpha < 1$) denotes a fraction of the total transmit power available for orthogonal transmission. In (13), $A_b = G A_d$ represents the mean power of the backhaul channel.

Proof: See Appendix B. ■

- Nonorthogonal scheme:

In this scenario, two users are receiving data in T_2 , i.e., one with a single MFemtocell and another directly with the BS. For a fair comparison, the BS transmit power is also shared equally between the MFemtocell and the direct transmission user. The required (E_b/N_0) to achieve the spectral efficiency, i.e., $C^{\text{non-orthg}}$, for the nonorthogonal scheme in the low-SNR regime is given by

$$\begin{aligned} \left(\frac{E_b}{N_0}\right)_{\text{dB}}^{\text{non-orthg}} &\approx 10 \log_{10} \\ &\times \left(\max \left\{ \frac{4 \ln 2}{(\alpha G + 1) A_d}, \frac{2 \ln 2}{(1 - \alpha) A_a + A_d} \right\} \right) \\ &+ \frac{3(G^2 \alpha^2 + 1) \kappa(|h_d|)}{(G \alpha + 1)^2} C^{\text{non-orthg}} \end{aligned} \quad (14)$$

where A_a denotes the mean power of the access channel.

Proof: See Appendix C. ■

B. High-SNR Regime

In the high-SNR regime, the required energy efficiency to obtain a specific spectral efficiency can be expressed as [28]

$$\frac{E_b}{N_0}_{\text{dB}} \approx \frac{C}{S_\infty} 10 \log_{10} 2 - 10 \log_{10}(C) + 3 \left(\frac{E_b}{N_0} \right)_{\text{penalty}} \quad (15)$$

where S_∞ is the slope of the spectral efficiency in the high-SNR regime in b/s/Hz/(3 dB) and is given by

$$S_\infty = \lim_{\text{SNR} \rightarrow \infty} \text{SNR} \dot{C}(\text{SNR}). \quad (16)$$

In (15), $(E_b/N_0)_{\text{penalty}}$ is the asymptotic penalty in the high-SNR regime and can be expressed as [28]

$$\left(\frac{E_b}{N_0}\right)_{\text{penalty}} = \lim_{\text{SNR} \rightarrow \infty} \left(\log_2(\text{SNR}) - \frac{\bar{C}(\text{SNR})}{S_\infty} \right). \quad (17)$$

1) *Direct Transmission:* The dependence between (E_b/N_0) and C^{direct} for the direct transmission link with the absence of the MFemtocell can be calculated as

$$\begin{aligned} \left(\frac{E_b}{N_0}\right)_{\text{dB}}^{\text{direct}} &\approx C^{\text{direct}} 10 \log_{10} 2 - 10 \log_{10}(C^{\text{direct}}) \\ &+ 10 \ln(A_d) + 2.5067. \end{aligned} \quad (18)$$

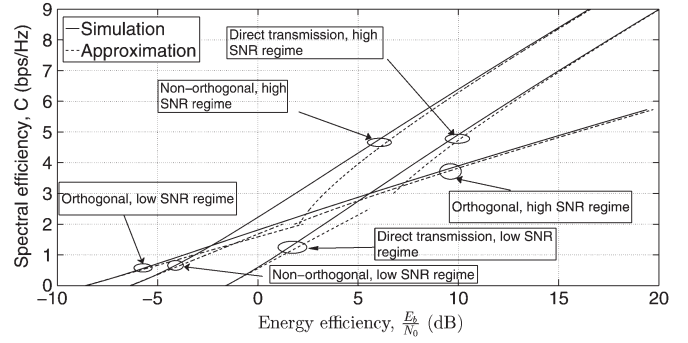


Fig. 3. Spectral efficiency versus energy efficiency for a link-level MFemtocell with orthogonal and nonorthogonal resource partitioning schemes.

Proof: See Appendix D. ■

2) *Orthogonal Scheme:* Assuming that the user is within close proximity to the respective MFemtocell, then the relationship between (E_b/N_0) and C^{orthg} is characterized by

$$\begin{aligned} \left(\frac{E_b}{N_0}\right)_{\text{dB}}^{\text{orthg}} &\approx C^{\text{orthg}} 10 \log_{10} 2 - 10 \log_{10}(C^{\text{orthg}}) \\ &+ \left(-\log_2(2\alpha G A_d) + \frac{\Upsilon}{\ln 2} \right) 10 \log_{10} 2 \end{aligned} \quad (19)$$

where Υ is the Euler–Mascheroni constant.

Proof: See Appendix E. ■

3) *Nonorthogonal Scheme:* Again, we assume here there are two users served by the BS and an MFemtocell at T_2 . The total power transmitted in both time slots is limited to P . The relationship between (E_b/N_0) and $C^{\text{non-orthg}}$ in the high-SNR regime is then characterized by

$$\begin{aligned} \left(\frac{E_b}{N_0}\right)_{\text{dB}}^{\text{non-orthg}} &\approx C^{\text{non-orthg}} 10 \log_{10} 2 - 10 \log_{10}(C^{\text{non-orthg}}) \\ &+ \left(-0.5 \log_2(\alpha G A_d) + \frac{\Upsilon}{\ln 2} \right) 10 \log_{10} 2. \end{aligned} \quad (20)$$

Proof: See Appendix F. ■

To verify the derived equations with different resource partitioning schemes, we performed simulations with a single BS, an MFemtocell, and two users. The distance between the MFemtocell and its user is much smaller than the distance between the MFemtocell and the BS. The macrocell user or the direct transmission user was placed far away from the MFemtocell so that the interference from the MFemtocell to the direct transmission user can be neglected or considered as background noise. In the nonorthogonal scheme, both users can receive data from the MFemtocell and the BS. Both A_d and A_a are equal to 1, whereas backhaul gain G is equal to 8 dB. Furthermore, α is equal to 70% for orthogonal and nonorthogonal schemes.

Fig. 3 presents the spectral/energy efficiency tradeoff for the direct, orthogonal, and nonorthogonal schemes. In the low-SNR regime, the orthogonal partitioning scheme provides better energy efficiency (i.e., needs less energy) than both the nonorthogonal partitioning scheme and the direct transmission scheme with the same spectral efficiency. However, the gap between

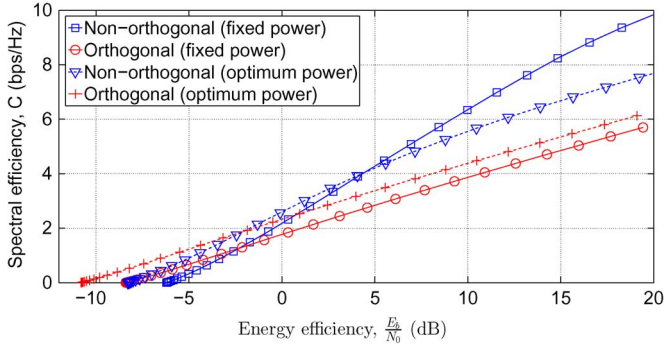


Fig. 4. Spectral efficiency versus energy efficiency for a link-level MFemto-cell with orthogonal and nonorthogonal resource partitioning schemes having different power control schemes.

the orthogonal and nonorthogonal partitioning schemes starts to decrease as we move to the high-SNR regime. The decrease in the gap is due to the fact that the slope of the orthogonal scheme is less than the slope of the nonorthogonal scheme. We can also notice that the direct transmission scheme has better energy efficiency than the orthogonal partitioning scheme when the spectral efficiency is more than 3 b/s/Hz. This is because when the underlying channel condition is good (high spectral efficiency), it is more energy efficient for the BS to transmit signals directly to a user with one time slot rather than to transmit to a user with an MFemto-cell.

Furthermore, in both SNR regimes, the nonorthogonal partitioning scheme provides better spectral efficiency than the direct transmission scheme with the same energy consumption because of the spectrum sharing between the BS and the MFemto-cell. As we can see, the simulation results match well the derived closed-form expressions in high- and low-SNR regimes.

The maximum link-level spectral efficiency can be achieved when backhaul spectral efficiency, i.e., C_b , and the access spectral efficiency, i.e., C_a , are equal [16]. In this case, the optimum value for the power fraction α^* can be calculated according to

$$\alpha^* = \frac{|h_a|^2}{|h_a|^2 + |h_b|^2}. \tag{21}$$

Thus, the spectral efficiency can be enhanced by using the optimum power fraction to allocate the power between the BS and the MFemto-cell. Fig. 4 shows the spectral/energy efficiency tradeoff for the two partitioning schemes using the optimum and fixed power allocation schemes. We can see that in the case of the orthogonal scheme, there is a 3-dB improvement in the energy efficiency by using the optimum power allocation compared with using the fixed power allocation. Furthermore, the slope of the spectral efficiency for the orthogonal scheme is not changed in both power allocation mechanisms. This is due to the fact that the slope does not depend on the power fraction α . We can also notice that when the spectral efficiency is less than 4 b/s/Hz, the nonorthogonal scheme provides better energy efficiency by adopting the optimum power allocation scheme rather than adopting the fixed power allocation scheme. However, when the spectral efficiency is larger than 4 b/s/Hz,

the nonorthogonal scheme needs more energy to achieve a given spectral efficiency by using the optimum power allocation scheme compared with using the fixed power allocation scheme. This is due to the fact that there is strong intracell interference from the BS to the users.

IV. SPECTRAL EFFICIENCY ANALYSIS FOR SYSTEM-LEVEL MOBILE FEMTOCELLS WITH MULTIUSER SCHEDULING

Here, we consider a system-level MFemto-cell network with one BS (single cell), multiple MFemto-cells, and multiple users. The spectrum is split into orthogonal resource blocks (RBs) for OFDMA-based cellular systems. These RBs are shared by different users by using opportunistic resource allocation in both frequency and time domains. Multiuser scheduling is assumed here, where the macrocell users and MFemto-cells are served over K RBs, which are indexed by $k = 1, \dots, K$, based on the well-known MAX-SINR and proportional fairness (PF) scheduling policies [37]. The BS and all MFemto-cells transmit with fixed power per RB. To support the opportunistic scheduling, the BS gathers the channel quality indicator from all users and MFemto-cells. The users within an MFemto-cell will feedback this information to the MFemto-cell only. By using the MAX-SINR scheduler, the BS will assign an RB k to a user n having the highest instantaneous rate at a subframe t , i.e.,

$$\bar{n}_k = \arg \max_{n \in \mathcal{N}} R_n(t, k), \quad k = 1, \dots, K \tag{22}$$

where $R_n(t, k) \propto \gamma_{n(D)}(t, k)$ in the orthogonal scheme (or $\hat{\gamma}_{n(D)}(t, k)$ in the nonorthogonal scheme) is the instantaneous achievable rate on RB k for user n , and $\arg \max f$ is an operator that gives the index at which vector f has the maximum value. In the PF scheduling case, the scheduler allocates RB k to a user $n \in \mathcal{N}$ according to the following criterion:

$$\bar{n}_k = \arg \max_{n \in \mathcal{N}} \frac{R_n(t, k)}{\bar{R}_n(t)} \quad k = 1, \dots, K \tag{23}$$

where $\bar{R}_n(t)$ is the average delivered rate in the past, which is measured over a fixed window of observation. It can be calculated using average filtering [37], which will be updated using the following formula:

$$\bar{R}_n(t) = \left(1 - \frac{1}{T}\right) \bar{R}_n(t-1) + \frac{1}{T} \sum_{k=1}^K R_n(t, k) d_n(t, k) \tag{24}$$

where T is the time window constant, and $d_n(t, k)$ is a binary indicator that is set to 1 if user n is scheduled on RB k at time t and to 0 otherwise.

The communication over the BS–MFemto-cell links takes place over a dedicated time–frequency zone, as shown in Fig. 2(a) and (b). Moreover, the same scheduling algorithm is used for the BS to schedule MFemto-cells and direct transmission users. Within the MFemto-cell j , it is assumed that the users (\mathcal{M}_j) are served according to a round-robin policy. In case of the orthogonal scheme, it is assumed that a fraction of the spectrum β , $0 < \beta < 1$, is exclusively allocated for direct transmissions in the second portion of the time, as shown in Fig. 2(a).

However, in the nonorthogonal scheme, the BS and MFemtocells can utilize the whole spectrum to serve their users, as shown in Fig. 2(b).

Achievable spectral efficiency on the direct transmission link on time t can be calculated as

$$C_d(t) = \begin{cases} \frac{1}{2B} \sum_{n \in \mathcal{N}} \sum_{k=1}^{\beta K} R_n(t, k) d_n(t, k), & \text{orthogonal} \\ \frac{1}{2B} \sum_{n \in \mathcal{N}} \sum_{k=1}^K R_n(t, k) d_n(t, k), & \text{non orthogonal.} \end{cases} \quad (25)$$

The achievable spectral efficiency on the access link can be given by

$$C_a^j(t) = \begin{cases} \frac{1}{2B} \sum_{m_j \in \mathcal{M}_j} \sum_{k=1}^{(1-\beta)K} R_{m_j}(t, k) d_{m_j}(t, k), & \text{orthogonal} \\ \frac{1}{2B} \sum_{m_j \in \mathcal{M}_j} \sum_{k=1}^K R_{m_j}(t, k) d_{m_j}(t, k), & \text{non orthogonal} \end{cases} \quad (26)$$

where $R_{m_j}(t, k)$ is the instantaneous achievable rate for an access user m . However, the rates on the access link between MFemtocells and their users are truncated by the achievable spectral efficiency of the backhaul link for MFemtocell j , i.e.,

$$C_b^j(t) = \frac{1}{2B} \sum_{k=1}^K R_j(t, k) d_j(t, k) \quad (27)$$

where $R_j(t, k)$ is the instantaneous achievable rate over the backhaul link for an MFemtocell j . As a result, the total system spectral efficiency (in b/s/Hz/cell) after allocating all RBs to the selected users, including MFemtocell users, can be calculated according to

$$C_{\text{sys}}(t) = \sum_{j=1}^J \min [C_b^j(t - \tau), C_a^j(t)] + C_d(t) \quad (28)$$

where τ is the time required to decode, buffer, and reencode the incoming data from the backhaul links. The first term in (28) stands for the achievable spectral efficiency of data flow from the BS to users through an MFemtocell, and the second term represents the spectral efficiency for direct transmission users. To get an efficient resource usage for MFemtocell deployment, the spectral efficiency over the backhaul and access links should be equal, i.e., $C_b^j(t - \tau) = C_a^j(t)$. It is worth mentioning that to improve the spectral efficiency, another form of spectrum reuse scheme can be adopted. For example, multiple MFemtocells can use a common set of subchannels simultaneously to serve their users. Both orthogonal and nonorthogonal resource partitioning schemes can benefit from MFemtocell spectrum reuse to improve spectral efficiency. This can only work, however, if multiple MFemtocells are located large distances apart or the coverage of each MFemtocell is limited to a small area by using a directive antenna.

A. Simulation Results and Discussions

The performance of the MFemtocell in the Long-Term Evolution (LTE) system is evaluated using a dynamic system-level

TABLE I
SIMULATION PARAMETERS

Parameter	BS-MFemtocell	BS-user	MFemtocell-user
Antenna height (m)	20	20	2
Shadowing (dB)	8	8	4
Antenna gain (dBi)	18	18	5
Bandwidth (MHz)	10	10	10
Transmit power (dBm)	46	46	35
Spectrum sharing (β)	100%	50%	50%
Time sharing	50%	50%	50%
Distance D (m)	≥ 40	≥ 50	≤ 15

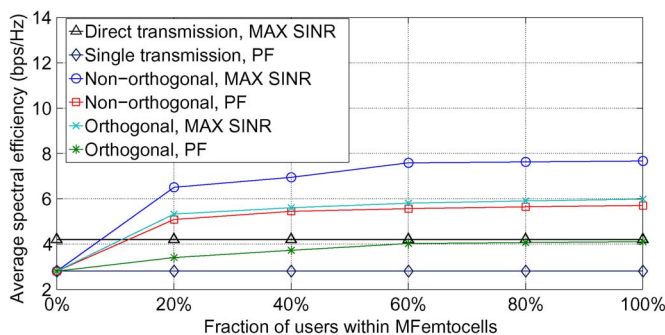


Fig. 5. Average spectral efficiency of system-level MFemtocells with multi-user scheduling and resource partitioning schemes, where $U = 40$, $K = 50$, $P_{\text{BS}} = 46$ dBm, $P_{\text{MF}} = 35$ dBm, and $G = 8$ dB.

simulator, which is compliant with the 3rd Generation Partnership Project LTE specification [38]. A frequency-selective fading channel with six taps is used. The LTE frame structure is considered, which consists of blocks of 12 contiguous subcarriers in the frequency domain and seven orthogonal frequency-division multiplexing symbols in the time domain. One subframe (1 ms) is regarded as a scheduling period. The simulations are based on the Monte Carlo method, which consists of multiple snapshots. In each snapshot, the direct transmission users are distributed randomly and independently within the coverage of the BS. In addition, each snapshot has 20 000 subframes, which are divided into units of ten. Each of the ten time slots are further divided equally so that the first five time slots are allocated to T_1 and that the second five time slots are allocated to T_2 . The carrier bandwidth is fixed at 10 MHz with 50 RBs. All users are equipped with a single antenna, whereas the MFemtocells have two antennas working in diversity mode. A full BS buffer is considered where there are always buffered data ready for transmission for each node. The users inside an MFemtocell experience 5-dB penetration loss when receiving a signal from the BS. The path loss between the BS and the direct user or the MFemtocell is calculated by $128.1 + 37.6 \log_{10}(D/1000)$, whereas the path loss between the MFemtocell and an access user within the vehicle is given by $127 + 30 \log_{10}(D/1000)$. Other relevant simulation parameters are summarized in Table I.

Fig. 5 compares the average spectral efficiency of the orthogonal and nonorthogonal partitioning schemes using MAX-SINR and PF scheduling algorithms in an MFemtocell-enhanced system as a function of a percentage of users that associate with MFemtocells. Here, it has been assumed that the total number of users, i.e., U , and MFemtocells, i.e., J , are assumed to be 50 and 3, respectively. The MFemtocells are mounted inside

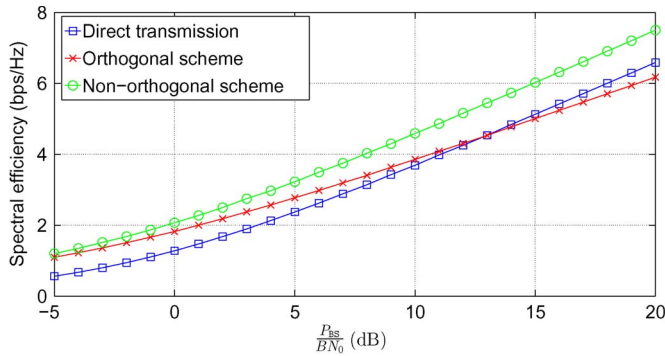


Fig. 6. Spectral efficiency as a function of (P_{BS}/BN_0) , $U = 40$, $K = 50$, $P_{BS} = 46$ dBm, $P_{MF} = 35$ dBm, and $G = 8$ dB.

busses that carry ten users each. The MFemtocells are randomly distributed within the coverage of the BS in each snapshot. Regardless of using either an orthogonal or a nonorthogonal partitioning scheme, adopting the concept of the MFemtocell has a positive impact on the overall spectral efficiency. In addition, increasing the percentage of users that communicate through the MFemtocell leads to an increase in the overall spectral efficiency in comparison with the case where all the users are communicating directly to the BS, i.e., $N = U$. This is because of the multiuser diversity gain, offered by opportunistic scheduling for users and the MFemtocells, as well as the backhaul gain over the direct transmission that the MFemtocell can offer. The simulation results demonstrate that there is a better spectral efficiency gain that can be achieved through sharing the spectrum between the BS and the MFemtocell in the same cell in the case of the nonorthogonal transmission scheme. Although the access users experience additional interference contributed from the BS, their performance does not get impacted in a noticeable way since they have a good-quality channel to the MFemtocell station with high signal power. We can consider the spectral efficiency with the MAX-SINR scheduler as an upper bound performance for MFemtocell systems because the BS always selects an MFemtocell and/or a user that has the best channel condition. However, it is noticeable that the gap between the MAX-SINR and PF scheduling algorithms in the nonorthogonal partitioning scheme is much larger than that in the orthogonal partitioning scheme. Although MAX-SINR scheduling would give a more consistent performance, it is at the cost of degrading the performance of cell-edge users. It is very important that MFemtocell deployment does not compromise the performance of the direct users; thus, PF scheduling is more suitable in this case.

Fig. 6 shows the system spectral efficiency of the two partitioning schemes as functions of transmit power of the BS. Here, we assume that there is one MFemtocell that is located 200 m apart from the BS and carries traffic for ten users. There are also 40 direct transmission users that are randomly located within the coverage of the BS. We can notice that both schemes provide better performance, as compared with the direct transmission reference system. However, when the BS transmit power is sufficiently high, i.e., when P_{BS}/BN_0 is larger than 14 dB, the direct transmission scheme offers better spectral efficiency than the orthogonal partitioning scheme.

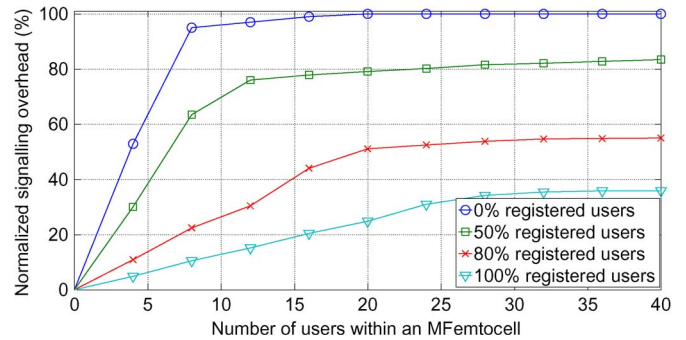


Fig. 7. Normalized signaling overhead as a function of the number of users within an MFemtocell, $M = 10$, and $K = 50$.

This is due to the fact that in the high-SNR regime, it is worth transmitting directly to a user using one time slot rather than using two time slots through an MFemtocell. This also means that the orthogonal partitioning scheme may not be suitable when the MFemtocells are moving near the BS.

In wireless communication systems, the BS will require some information from the end users to allocate the radio resources efficiently or make handover operation. The end users in LTE cellular systems, for instance, are needed to feedback their downlink channel quality to the BS to support the channel-dependent scheduling and link adaptation. This information is forwarded to the BS over dedicated uplink control signaling channels. More control signaling means more sacrifice in system performance. As mentioned earlier, the MFemtocell can significantly decrease the uplink control signaling information of the direct transmission users. To demonstrate this fact, we analyze the uplink control signaling overhead in LTE cellular systems with and without MFemtocell deployment. The signaling overhead is the percentage of required control signaling with respect to the reference direct transmission. Here, we use discrete adaptive modulation schemes, including quaternary phase-shift keying, 16 quadrature amplitude modulation (QAM), and 64-QAM. Each modulation scheme with a different coding rate is supported when the uplink SNR is above a predefined SNR threshold. The SNR thresholds have been taken from [39]. The size of the control signal in symbols per subframe is determined by [39]

$$S_z = \left[\frac{N \times S_{ctr}}{B_s} \right] \quad (29)$$

where N is the number of control signaling bits, and B_s and S_{ctr} are bits per symbol and coding rate of the selected modulation and coding scheme, respectively.

Fig. 7 presents the reduction in the control signaling in the uplink backhaul link as a function of the number of users, within a vehicle, that communicate through an MFemtocell. As it is clearly shown, the greater the percentage of users that register to an MFemtocell, the greater the reduction in the control signaling overhead, compared with that of the reference direct transmission scheme, i.e., 0% of users communicate through an MFemtocell. Thus, with MFemtocell deployment, all users within an MFemtocell only need to send their control signaling to the MFemtocell rather than to the BS. The MFemtocell will cut off all these messages and send only its feedback to the

BS. The control signaling information between users and the MFemtocell does not add to the total system control signaling overhead. The amount of reduction in signaling overhead can then be replaced with useful data and, hence, improvement in the users and system throughput. We can also notice that for any case of registered users, the control signal overhead tends to be saturated after a certain number of users within the MFemtocells. This is due to the fact that there is a limitation to the number of users that can use the uplink control channel. In the case of 50% (or 80%) of registered users, the control signaling overhead consists of the control signal that comes from both the direct and access users.

V. CONCLUSION

In this paper, the spectral efficiency and energy efficiency for MFemtocell systems have been investigated. It has been shown that the energy efficiency can be enhanced by using the nonorthogonal scheme for the moderate and high SNR values. The chapter has also investigated the spectral efficiency of two resource partitioning schemes in a system-level MFemtocell in the presence of opportunistic scheduling. It has been shown that the spectral efficiency can be improved by employing the nonorthogonal partitioning scheme to share the spectrum between the BS and MFemtocells. The purpose of using the nonorthogonal transmission scheme is that the access users are considered indoor and that they are within close proximity to the MFemtocell station. Although the nonorthogonal scheme avoids the interference, it comes at the price of reduced spectral efficiency. This makes the nonorthogonal transmission scheme more attractive than the orthogonal transmission scheme, even in the absence of any kind of coordination between the BS and MFemtocells.

This paper has also demonstrated that the implementation of MFemtocells can reduce the signaling overhead, resulting in an enhanced system performance. Therefore, the MFemtocell can be considered as a potential candidate technology to be deployed in 5G mobile cellular systems to increase the performance of users within vehicles and of the overall system.

APPENDIX A
DERIVATION OF (12)

The achievable spectral efficiency C of the direct transmission scheme is given by

$$C = \mathbb{E} \left[\log_2 \left(1 + \frac{|h_d|^2 P_{BS}}{BN_0} \right) \right] \quad (30)$$

where $\mathbb{E}[\cdot]$ is the expectation operator. If we assume that $|h_d|$ follows a Rayleigh fading distribution, $|h_d|^2$ has an exponential distribution (i.e., $e^{-A_d x} \forall x > 0$) with $\mathbb{E}[|h_d|^2] = A_d$ denoting the mean power of the channel. By letting $\text{SNR} \equiv (P_{BS}/BN_0)$, (10) and (11) can be written as

$$S_0 = \frac{2}{\kappa(|h_d|)} \quad (31)$$

$$\left(\frac{E_b}{N_0} \right)_{\min} = \frac{\ln 2}{\mathbb{E}[|h_d|^2]} = -1.59 + 10 \log_{10}(A_d) \text{ dB} \quad (32)$$

respectively. In (31), $\kappa(|x|)$ is the kurtosis of random variable x , which is defined as [28]

$$\kappa(|x|) = \frac{\mathbb{E}[|x|^4]}{\mathbb{E}[|x|^2]^2}. \quad (33)$$

For Rayleigh fading, $\kappa(|x|) = 2$, and consequently, $S_0 = 1$ [28]. We can notice that $(E_b/N_0)_{\min}$ is the same in additive white Gaussian noise and Rayleigh fading channels, but the slope, i.e., S_0 , has a 2.5-dB difference. Applying (31) and (32) into (9), (12) is then obtained.

APPENDIX B
DERIVATION OF (13)

In Fig. 2(a), the MFemtocell will receive the data in T_1 and then transmit the data again to the user in T_2 . The achievable spectral efficiency C over two time slots is limited to minimum capacity, i.e.,

$$C = \min\{C_b, C_a\} \quad (34)$$

where C_b and C_a are the spectral efficiency of the backhaul and access links, respectively. However, by considering that the distance between the access user and the MFemtocell is much shorter than the distance between the BS and the MFemtocell, we can then expect that the spectral efficiency is always limited by the backhaul spectral efficiency. The spectral efficiency of the backhaul link can be calculated as

$$C_b = \frac{1}{2} \mathbb{E} \left[\log_2 \left(1 + \frac{\alpha |h_b|^2 P}{BN_0} \right) \right]. \quad (35)$$

The factor 1/2 in (35) is due to the fact that the transmission to the end user occurs in two successive time slots. Moreover, both the BS and the MFemtocell transmit only half of the time. In (10), $(E_b/N_0)_{\min}$ can be calculated as

$$\left(\frac{E_b}{N_0} \right)_{\min} = \left(\frac{E_b}{N_0} \right)_{\min}^b = \frac{2 \ln 2}{\alpha G A_d}. \quad (36)$$

The minimum normalized energy is characterized by the backhaul gain and the fraction of the transmit power allocated to the BS. By substituting (11), the slope of the spectral efficiency for the orthogonal scheme is expressed as

$$S_0 = (S_0)_b = \frac{1}{\kappa(|h_d|)}. \quad (37)$$

Substituting (36) and (37) into (9), (13) can be obtained.

APPENDIX C
DERIVATION OF (14)

In the nonorthogonal partitioning scheme, both the BS and the MFemtocell can share the spectrum of T_2 to serve direct transmission and access users but at the price of introducing additional interference to both users. The access user, however, would experience the burden of the majority of the interference. Hence, the impact of the MFemtocell interference on the direct transmission users can be ignored and considered as

background noise by assuming that the MFemtocell and the user are of long distance apart. Nevertheless, the achievable spectral efficiency is equal to

$$C_{\text{non-orthog}} = \min\{C_b, C_a\} + C_d \quad (38)$$

where $C_d = (1/2)\mathbb{E}[\log_2(1 + (|h_d|^2 P_{\text{BS}}/2BN_0))]$ is the spectral efficiency of the direct transmission link. Here, it has been assumed that the transmit power of the BS is shared equally between the MFemtocell and the direct transmission user. Again, the factor 1/2 is because the direct transmission happens only in the second time slot. The spectral efficiency over the access link, i.e., C_a , and the backhaul link are given by

$$\begin{aligned} C_a &= \frac{1}{2}\mathbb{E}\left[\log_2\left(1 + \frac{(1-\alpha)|h_a|^2 P}{|h_d|^2 P_{\text{BS}} + BN_0}\right)\right] \\ &= \frac{1}{2}\mathbb{E}\left[\log_2\left(1 + \frac{(1-\alpha)|h_a|^2 \text{SNR}}{|h_d|^2 \text{SNR} + 1}\right)\right] \end{aligned} \quad (39)$$

$$C_b = \frac{1}{2}\mathbb{E}\left[\log_2\left(1 + \frac{\alpha|h_b|^2 P}{2BN_0}\right)\right] \quad (40)$$

respectively. Substituting (38)–(40) into (10), $(E_b/N_0)_{\min}$ can be obtained as (41), shown at the bottom of the page, where $A_a = \mathbb{E}[|h_a|^2]$ denotes the mean power of the access channel. The wideband slope S_0 can be obtained by substituting (38)–(40) into (11) and can be expressed by (42), shown at the bottom of the page. Putting (41) and (42), into (9) leads to (14).

APPENDIX D DERIVATION OF (18)

For the direct transmission user, in the high-SNR regime, the slope of spectral efficiency is equivalent to

$$S_\infty = \lim_{\text{SNR} \rightarrow \infty} \text{SNR} \frac{\partial (\log_2(1 + |h_d|^2 \text{SNR}))}{\partial \text{SNR}}. \quad (43)$$

The asymptotic penalty in the high-SNR regime in (15) can be calculated as

$$\begin{aligned} \left(\frac{E_b}{N_0}\right)_{\text{penalty}} &= \lim_{\text{SNR} \rightarrow \infty} \log_2\left(\frac{\text{SNR}}{1 + |h_d|^2 \text{SNR}}\right) \\ &= -\mathbb{E}[\log_2(|h_d|^2)]. \end{aligned} \quad (44)$$

Since $|h_d|^2$ has an exponential probability density function, i.e., $e^{-A_d x}$, (44) can be rewritten as

$$\left(\frac{E_b}{N_0}\right)_{\text{penalty}} = -\int_0^\infty e^{-A_d x} \log_2(x) dx = \frac{\gamma}{\ln 2} + \ln(A_d) \quad (45)$$

where γ is the Euler–Mascheroni constant. Putting (43) and (45) into (15), (18) can be obtained.

APPENDIX E DERIVATION OF (19)

For the orthogonal scheme, the slope in the high-SNR regime is equal to (46), shown at the bottom of the page, whereas $(E_b/N_0)_{\text{penalty}}$ is given by (47), shown at the top of the next page. Substituting (46) and (47) into (15), (19) can be obtained.

$$\begin{aligned} \left(\frac{E_b}{N_0}\right)_{\min} &= \frac{\ln 2}{\frac{\partial \left(\frac{1}{2}\mathbb{E}\left[\min\left\{\log_2\left(1 + \frac{(1-\alpha)|h_a|^2 \text{SNR}}{|h_d|^2 \text{SNR} + 1}\right), \log_2(1 + 0.5\alpha|h_b|^2 \text{SNR})\right\} + \log_2(1 + |h_d|^2 \text{SNR})\right]\right)}{\partial \text{SNR}}} \\ &= \max\left\{\frac{4 \ln 2}{(\alpha G + 1)A_d}, \frac{2 \ln 2}{(1-\alpha)A_a + A_d}\right\}, \quad \text{SNR} = 0 \end{aligned} \quad (41)$$

$$\begin{aligned} S_0 &= \frac{\frac{\partial \left(\mathbb{E}\left[\min\left\{\log_2\left(1 + \frac{(1-\alpha)|h_a|^2 \text{SNR}}{|h_d|^2 \text{SNR} + 1}\right), \log_2(1 + 0.5\alpha|h_b|^2 \text{SNR})\right\} + \log_2(1 + |h_d|^2 \text{SNR})\right]\right)}{\partial \text{SNR}}}{\frac{\partial^2 \left(\mathbb{E}\left[\min\left\{\log_2\left(1 + \frac{(1-\alpha)|h_a|^2 \text{SNR}}{|h_d|^2 \text{SNR} + 1}\right), \log_2(1 + 0.5\alpha|h_b|^2 \text{SNR})\right\} + \log_2(1 + |h_d|^2 \text{SNR})\right]\right)}{\partial \text{SNR}^2}} \\ &= \frac{(G\alpha + 1)^2}{(G^2\alpha^2 + 1)\kappa(|h_d|)}, \quad \text{SNR} = 0 \end{aligned} \quad (42)$$

$$S_\infty = \lim_{\text{SNR} \rightarrow \infty} \text{SNR} \frac{\partial (\min\{\frac{1}{2}\log_2(1 + 2\alpha G|h_d|^2 \text{SNR}), \frac{1}{2}\log_2(1 + 2(1-\alpha)|h_a|^2 \text{SNR})\})}{\partial \text{SNR}} \quad (46)$$

$$\begin{aligned} \left(\frac{E_b}{N_0}\right)_{\text{penalty}} &= \max \left\{ \lim_{\text{SNR} \rightarrow \infty} \log_2 \left(\frac{\text{SNR}}{1 + 2\alpha G|h_d|^2 \text{SNR}} \right), \lim_{\text{SNR} \rightarrow \infty} \log_2 \left(\frac{\text{SNR}}{1 + 2(1-\alpha)|h_a|^2 \text{SNR}} \right) \right\} \\ &= \max \left\{ - \left(\log_2(2\alpha G A_d) + \frac{\gamma}{\ln 2} \right), - \left(\log_2(2(1-\alpha)A_a) + \frac{\gamma}{\ln 2} \right) \right\} \end{aligned} \quad (47)$$

$$S_\infty = \lim_{\text{SNR} \rightarrow \infty} \frac{\text{SNR} \partial \left(\mathbb{E} \left[\min \left\{ \log_2 \left(1 + \frac{(1-\alpha)|h_a|^2 \text{SNR}}{|h_d|^2 \text{SNR} + 1} \right), \log_2 \left(1 + \alpha|h_b|^2 \text{SNR} \right) \right\} + \log_2 \left(1 + |h_d|^2 \text{SNR} \right) \right] \right)}{\partial \text{SNR}} \quad (48)$$

APPENDIX F DERIVATION OF (20)

For the nonorthogonal scheme, the slope of the spectral efficiency is given by (48), shown at the top of the page. Moreover, (17) can be calculated as

$$\left(\frac{E_b}{N_0}\right)_{\text{penalty}} = -0.5 \log_2(\alpha G A_d) + \frac{\gamma}{\ln 2}. \quad (49)$$

Substituting (48) and (49) into (15), (20) can be obtained.

REFERENCES

- [1] S.-P. Yeh *et al.*, "Capacity and coverage enhancement in heterogeneous networks," *IEEE Wireless Commun.*, vol. 18, no. 3, pp. 32–38, Jun. 2011.
- [2] A. Damnjanovic *et al.*, "A survey on 3GPP heterogeneous networks," *IEEE Wireless Commun.*, vol. 18, no. 3, pp. 10–21, Jun. 2011.
- [3] V. Chandrasekhar, J. Andrews, and A. Gatherer, "Femtocell networks: A survey," *IEEE Commun. Mag.*, vol. 46, no. 9, pp. 59–67, Sep. 2008.
- [4] D. Feng *et al.*, "A survey of energy-efficient wireless communications," *IEEE Commun. Mag.*, vol. 15, no. 1, pp. 167–178, 1st Quart. 2013.
- [5] F. Haider *et al.*, "Spectral efficiency analysis of mobile femtocell based cellular systems," in *Proc. IEEE ICCT*, Jinan, China, Sep. 2011, pp. 347–351.
- [6] C.-X. Wang *et al.*, "Cellular architecture and key technologies for 5G wireless communication networks," *IEEE Commun. Mag.*, vol. 52, no. 2, pp. 122–130, Feb. 2014.
- [7] T. Elkourdi and O. Simeone, "Femtocell as a relay: An outage analysis," *IEEE Trans. Wireless Commun.*, vol. 10, no. 12, pp. 4204–4213, Dec. 2011.
- [8] Y. Sui *et al.*, "Moving cells: A promising solution to boost performance for vehicular users," *IEEE Commun. Mag.*, vol. 51, no. 6, pp. 62–68, Jun. 2013.
- [9] F. Haider, M. Dianati, and R. Tafazolli, "A simulation based study of mobile femtocell assisted LTE networks," in *Proc. IEEE IWCMC*, Istanbul, Turkey, Jul. 2011, pp. 2198–2203.
- [10] M. Qutqut, M. Feteiha, and H. S. Hassanein, "Outage probability analysis of mobile small cells over LTE-A networks," in *Proc. IEEE IWCMC*, Aug. 2014, pp. 1045–1050.
- [11] M. H. Qutqut, "Mobile small cells in cellular heterogeneous networks," Ph.D. dissertation, Queen's Univ., Kingston, ON, Canada, Sep. 2014, [Online]. Available: <http://qspace.library.queensu.ca/handle/1974/12538>
- [12] M. Qutqut, F. Al-Turjman, and H. S. Hassanein, "MFW: Mobile femtocells utilizing Wi-Fi: A data offloading framework for cellular networks using mobile femtocells," in *Proc. IEEE ICC*, Jun. 2013, pp. 5020–5024.
- [13] "Network sharing: Architecture and functional description (Release 13)," Third-Generation Partnership Project, Sophia Antipolis Cedex, France, 3GPP TS 23.251 V13.1.0, Mar. 2015.
- [14] C.-X. Wang *et al.*, "Cooperative MIMO channel models: A survey," *IEEE Commun. Mag.*, vol. 48, no. 2, pp. 80–87, Feb. 2010.
- [15] D. Soldani and S. Dixit, "Wireless relays for broadband access," *IEEE Commun. Mag.*, vol. 46, no. 3, pp. 58–66, Mar. 2008.
- [16] A. Bou Saleh *et al.*, "Performance of amplify-and-forward and decode-and-forward relays in LTE-advanced," in *Proc. IEEE VTC—Fall*, Sep. 2009, pp. 1–5.
- [17] O. Oyman, "Opportunistic scheduling and spectrum reuse in relay-based cellular networks," *IEEE Trans. Wireless Commun.*, vol. 9, no. 3, pp. 1074–1085, Mar. 2010.
- [18] H. Claussen, "Performance of macro and co-channel femtocells in a hierarchical cell structure," in *Proc. IEEE PIMRC*, Sep. 2007, pp. 1–5.
- [19] I. Guvenc, M.-R. Jeong, F. Watanabe, and H. Inamura, "A hybrid frequency assignment for femtocells and coverage area analysis for co-channel operation," *IEEE Commun. Lett.*, vol. 12, no. 12, pp. 880–882, Dec. 2008.
- [20] Y. Bai, J. Zhou, and L. Chen, "Hybrid spectrum usage for overlaying LTE macrocell and femtocell," in *Proc. IEEE GLOBECOM*, Dec. 2009, pp. 1–6.
- [21] Y. Bai, J. Zhou, and L. Chen, "Hybrid spectrum sharing for coexistence of macrocell and femtocell," in *Proc. IEEE ICCTA*, Oct. 2009, pp. 162–166.
- [22] C. Han *et al.*, "Green radio: Radio techniques to enable energy efficient wireless networks," *IEEE Commun. Mag.*, vol. 49, no. 6, pp. 46–54, Jun. 2011.
- [23] I. Ku, C.-X. Wang, and J. S. Thompson, "Spectral–energy efficiency trade-off in relay-aided cellular networks," *IEEE Trans. Wireless Commun.*, vol. 12, no. 10, pp. 4970–4982, Oct. 2013.
- [24] X. Hong, Y. Jie, C.-X. Wang, J. Shi, and X. Ge, "Energy–spectral efficiency trade-off in virtual MIMO cellular systems," *IEEE J. Sel. Areas Commun.*, vol. 31, no. 10, pp. 2128–2140, Oct. 2013.
- [25] X. Hong, J. Wang, C.-X. Wang, and J. Shi, "Cognitive radio in 5G: A perspective on energy–spectral efficiency trade-off," *IEEE Commun. Mag.*, vol. 52, no. 7, pp. 46–53, Jul. 2014.
- [26] F. Haider *et al.*, "Spectral and energy efficiency analysis for cognitive radio networks," *IEEE Trans. Wireless Commun.*, vol. 14, no. 6, pp. 2969–2980, Jun. 2015.
- [27] S. Verdú, "Spectral efficiency in the wideband regime," *IEEE Trans. Inf. Theory*, vol. 48, no. 6, pp. 1319–1343, Jun. 2002.
- [28] S. Shamai and S. Verdú, "The impact of frequency-flat fading on the spectral efficiency of CDMA," *IEEE Trans. Inf. Theory*, vol. 47, no. 4, pp. 1302–1327, May 2001.
- [29] A. Lozano, A. Tulino, and S. Verdú, "Multiple-antenna capacity in the low-power regime," *IEEE Trans. Inf. Theory*, vol. 49, no. 10, pp. 2527–2544, Oct. 2003.
- [30] Y. Yao, X. Cai, and G. Giannakis, "On energy efficiency and optimum resource allocation of relay transmissions in the low-power regime," *IEEE Trans. Wireless Commun.*, vol. 4, no. 6, pp. 2917–2927, Nov. 2005.
- [31] J. Gomez-Vilardebo, A. Perez-neira, and M. Najar, "Energy efficient communications over the AWGN relay channel," *IEEE Trans. Wireless Commun.*, vol. 9, no. 1, pp. 32–37, Jan. 2010.
- [32] X. Cai, Y. Yao, and G. Giannakis, "Achievable rates in low-power relay links over fading channels," *IEEE Trans. Commun.*, vol. 53, no. 1, pp. 184–194, Jan. 2005.
- [33] O. Oyman and M. Win, "Power–bandwidth trade-off in multiuser relay channels with opportunistic scheduling," in *Proc. ALLERTON*, Urbana-Champaign, IL, USA, Sep. 2008, pp. 72–78.
- [34] N. Jindal, "High SNR analysis of MIMO broadcast channels," in *Proc. ISIT*, Sep. 2005, pp. 2310–2314.

- [35] A. Lozano, A. Tulino, and S. Verdu, "High-SNR power offset in multiantenna communication," *IEEE Trans. Inf. Theory*, vol. 51, no. 12, pp. 4134–4151, Dec. 2005.
- [36] F. Haider *et al.*, "Spectral–energy efficiency trade-off in cognitive radio networks with peak interference power constraints," in *Proc. IEEE ICCT*, Jinan, China, Sep. 2011, pp. 3682–372.
- [37] A. Jalali, R. Padovani, and R. Pankaj, "Data throughput of CDMA-HDR: A high efficiency–high data rate personal communication wireless system," in *Proc. IEEE VTC—Spring*, Tokyo, Japan, May 2000, pp. 1854–1858.
- [38] "Physical layer aspects for evolved UTRA (Release 7)," Third-Generation Partnership Project, Sophia Antipolis, France, 3GPP TS 25.814 V7.1.0, Sep. 2006.
- [39] "Simulation results: Linkage between PUSCH and amount of resources for control on PUSCH," Third-Generation Partnership Project, Sophia Antipolis, France, 3GPP WG1 R1-081853, May 2008.



Fourat Haider received the Bachelor's degree in electrical and electronic engineering/communication engineering from the University of Technology, Iraq, Baghdad, Iraq, in 2004 and the M.Sc. degree (with distinction) from Brunel University, London, U.K., in 2009. He is currently working toward the Ph.D. degree with Heriot-Watt University, Edinburgh, U.K., and the University of Edinburgh.

From 2005 to 2007, he was a Senior Network Engineer with AsiaCell company (a mobile operator in Iraq). In 2009, he joined a European project (predrive project) with the University of Surrey, Guildford, U.K., to develop a high-level-architecture-based simulation integration. He has also been working as an RAN strategy and architecture Engineer with Hutchison 3G U.K., Maidenhead, U.K. His main research interests include spectral-efficiency–energy-efficiency tradeoff, wireless channel capacity analysis, small cells, femtocells and mobile femtocells, and conventional and massive multiple-input–multiple-output systems.

Mr. Haider received the Best Paper Awards at the 2011 IEEE International Conference on Communication Technology.



Cheng-Xiang Wang (S'01–M'05–SM'08) received the B.Sc. and M.Eng. degrees in communication and information systems from Shandong University, Jinan, China, in 1997 and 2000, respectively, and the Ph.D. degree in wireless communications from Aalborg University, Aalborg, Denmark, in 2004.

Since 2005, he has been with Heriot-Watt University, Edinburgh, U.K., where he was promoted to Professor in 2011. He is also an Honorary Fellow with the University of Edinburgh, and a Chair/Guest Professor with Shandong University and Southeast

University, Nanjing, China. From 2001 to 2005, he was a Research Fellow with the University of Agder, Grimstad, Norway. In 2004, he was a Visiting Researcher with Siemens AG-Mobile Phones, Munich, Germany. From 2000 to 2001, he was a Research Assistant with Hamburg University of Technology, Hamburg, Germany. He is the Editor of one book. He has published one book chapter and over 210 papers in refereed journals and conference proceedings. His research interests include wireless channel modeling and simulation, green communications, cognitive radio networks, vehicular communication networks, massive multiple-input–multiple-output systems, and fifth-generation wireless communications.

Dr. Wang is a Fellow of the Institution of Engineering and Technology and the Higher Education Academy and a member of the Engineering and Physical Research Council Peer Review College. He has served as an Editor for eight international journals, including the IEEE TRANSACTIONS ON VEHICULAR TECHNOLOGY (since 2011) and the IEEE TRANSACTIONS ON WIRELESS COMMUNICATIONS (2007–2009). He was the lead Guest Editor for the IEEE JOURNAL ON SELECTED AREAS IN COMMUNICATIONS, Special Issue on Vehicular Communications and Networks. He has served as a Technical Program Committee (TPC) Member, a TPC Chair, and a General Chair for more than 70 international conferences. He received Best Paper Awards from the 2010 IEEE Global Telecommunications Conference, the 2011 IEEE International Conference on Communication Technology, the 2012 International Conference on ITS Telecommunications, and the 2013 IEEE Vehicular Technology Conference (Spring).



Bo Ai (M'00–SM'10) received the M.S. and Ph.D. degrees from Xidian University, Xi'an, China, in 2002 and 2004, respectively.

In 2007, he was an Excellent Postdoctoral Research Fellow with Tsinghua University, Beijing, China. He is currently a Professor and an Advisor of Ph.D. candidates with Beijing Jiaotong University, where he is also the Deputy Director of the State Key Laboratory of Rail Traffic Control and Safety. He is also with the Engineering College, Armed Police Force, Xi'an. He has authored or coauthored six

books and over 170 scientific research papers and holds 26 invention patents in his research areas. His interests include the research and applications of orthogonal frequency-division multiplexing techniques, high-power amplifier linearization techniques, radio propagation and channel modeling, global systems for mobile communications for railway systems, and long-term evolution for railway systems.

Dr. Ai is a Fellow of The Institution of Engineering and Technology. He was a Cochair or a Session/Track Chair for many international conferences, such as the Ninth International Heavy Haul Conference (2009); the 2011 IEEE International Conference on Intelligent Rail Transportation; the 2011 International ICST Workshop on Wireless Communications for High Speed Rail; the 2012 IEEE International Symposium on Consumer Electronics; the 2013 International Conference on Wireless, Mobile, and Multimedia; the 2013 IEEE Green HetNet; and the IEEE 78th Vehicular Technology Conference (2014). He is an Associate Editor of the IEEE TRANSACTIONS ON CONSUMER ELECTRONICS and an Editorial Committee Member of the *Wireless Personal Communications* journal. He has received many awards, such as the Qiushi Outstanding Youth Award from the HongKong Qiushi Foundation, the New Century Talents from the Chinese Ministry of Education, the Zhan Tianyou Railway Science and Technology Award from the Chinese Ministry of Railways, and the Science and Technology New Star from the Beijing Municipal Science and Technology Commission.



Harald Haas (S'98–M'03) received the Ph.D. degree from the University of Edinburgh, Edinburgh, U.K., in 2001.

He is currently the Chair of Mobile Communications with the University of Edinburgh. He is a Cofounder and the Chief Scientific Officer with pureLiFi Ltd. He has published 300 conference and journal papers, including a paper in *Science*. He holds 31 patents and has more than 30 pending patent applications. His main research interests are in optical wireless communications, hybrid optical

wireless and radio-frequency communications, spatial modulation, and interference coordination in wireless networks.

Dr. Haas first introduced and coined spatial modulation and Li-Fi. Li-Fi was listed among the 50 best inventions in *TIME Magazine* in 2011. He was an invited speaker at TED Global 2011, and his talk has been watched online more than 1.5 million times. He co-received the Best Paper Award at the IEEE Vehicular Technology Conference in Las Vegas, NV, USA, in 2013 and in Glasgow, U.K., in 2015 and the EURASIP Best Paper Award for the *Journal on Wireless Communications and Networking* in 2015. In 2012, he was the only recipient of the prestigious Established Career Fellowship from the Engineering and Physical Sciences Research Council (EPSRC) within Information and Communications Technology in the U.K. He also received the Tam Dalyell Prize 2013 from the University of Edinburgh for excellence in engaging the public with science. In 2014, he was selected by the EPSRC as one of the ten Recognizing Inspirational Scientists and Engineers (RISE) Leaders.



Erol Hepsaydir received the B.Sc. and M.Sc. degrees in electronics engineering from the Middle East Technical University, Ankara, Turkey, in 1985 and 1987, respectively, and the Ph.D. degree in telecommunications from the University of Technology Sydney, Australia, in 2001.

He is currently the Head of Radio and Devices Strategy with Hutchison 3G U.K., Maidenhead, U.K. He has been working in the cellular mobile industry for 22 years. He has worked for various mobile operators as a Network Technologist. He has recently

been appointed as a Royal Academy of Engineering Visiting Professor with the University of Kent, Kent, U.K. His earlier research involved the design and development of communications systems. His current work concerns next-generation mobile network developments and the analysis of new mobile technologies.

Dr. Hepsaydir is the IF&E Chair of the 2015 IEEE International Conference on Communications.